Biomedical Signal Processing and Control 64 (2021) 102230

Contents lists available at ScienceDirect

Biomedical Signal Processing and Control

journal homepage: www.elsevier.com/locate/bspc

Quality Aware Compression of Multilead Electrocardiogram Signal using 2-mode Tucker Decomposition and Steganography

Soumyendu Banerjee *, Girish Kumar Singh

Department of Electrical Engineering, Indian Institute of Technology Roorkee, Uttarakhand, Roorkee-247667, India

ARTICLE INFO

Keywords:
3D beat tensor
Tucker decomposition
Principal component analysis
Particle swarm optimization
Multi agent supervised learning system
Steganography

ABSTRACT

In this article, a quality controlled compression of multilead electrocardiogram (MECG) is proposed, based on tensor analysis, and implemented upon 3D beat tensor of MECG. To reduce computational complications and execution time, a new approach of principal component analysis (PCA), based on 2-mode Tucker Decomposition, is introduced. In order to maintain relevant features of MECG after reconstruction, multi agent supervised learning system (MASLS) based optimal quantization of each fiber of core tensor is introduced, to limit the percentage root mean squared difference (PRD) within a specified value, maintaining high compression ratio (CR). The MASLS is previously trained offline, using features of tensor fibers, along with optimized quantization levels of those fibers, obtained from a particle swarm optimization (PSO), as reference. In addition, to hide patient's confidential information, steganography is performed within the core tensor followed by generation of a' secret key', which is necessary, while decrypting those information during reconstruction. The whole algorithm is implemented on several MECG records, available in PTB Diagnostic ECG database, and compression result is compared by formation of *n*-beat tensor separately, using '*n*' number of successive ('*n*' = 5, 10 and 15) beats. After testing on 547 data, average CR of 22, 41.5, 55.4, PRD of 3.62, 4.96, 5.59 and PRD normalized (PRDN) of 3.61, 4.94, 5.57 are achieved for 5, 10, 15-beat tensor, respectively. This proposed algorithm has provided superior result as compared to recently published works on MECG data compression.

1. Introduction

The Electrocardiogram (ECG) is one of the most important bio-electric signal, which represents the variation of bio-potentials caused by rhythmic contraction and relaxation of heart muscle [1]. A multilead ECG (MECG) is basically continuous recording of 12 simultaneous ECG leads, which provide more information related to cardiac functionality than single lead measurement. Continuous monitoring of MECG data needs huge memory space (2 gigabyte a day/1 kHz sampling frequency and 16 bit data resolution) to store for further examination. Thus in order to use memory efficiently, data compression is necessary. Also for tele-monitoring applications, channel efficiency can be sufficiently increased, if the compressed data is sent in spite of sending raw ECG data, directly after recording [2].

Being a highly noisy signal, before any kind of processing, the raw ECG data is always needed to be filtered to eliminate high frequency noises. Wavelet transform (WT) [3], along with hill climbing topology [4,5] provided a great result regarding filtering ECG data, by decomposing the signal into various frequency subbands to neglect high frequency coefficients. Due to the presence of internal coherency of MECG signal, data reduction can be performed by reducing mainly three types of redundancies viz. interbeat (within each beat in single lead), intrabeat (within a single beat) and interlead (within various leads of MECG) redundancy. In single lead data compression approaches [6], mainly interbeat or intrabeat or both redundancies were reduced. Time domain approach of data reduction causes lower CR and higher reconstruction error. But various transformed domain approaches like, discrete cosine transform (DCT), Walsh transform, Karhunen–Loève theorem (KLT) etc. provide higher CR and lower error, as desired [7,8]. In most of the published works, data compression process was initiated by R-peaks detection [9]. Software detection of QRS complex [10] helps in beat detection and feature classification, which play important role for further computation.

For MECG data compression, mainly transformed domain techniques e.g. linear prediction, DCT, KLT were used [11]. An improvement of linear predication was reflected by using discrete wavelet transform (DWT) [12]. J. Wei et al. [13] implemented the singular value decomposition (SVD) on MECG data by selecting proper singular vectors and

* Corresponding author.
E-mail address: banerjeesoumyendu@gmail.com (S. Banerjee).

https://doi.org/10.1016/j.bspc.2020.102230
Received 17 June 2020; Received in revised form 22 August 2020; Accepted 18 September 2020
Available online 29 October 2020

achieved CR of 10 and PRD of 1.18. Principal component analysis (PCA) is a powerful dimension reduction tool [14–15] using which, data compression can be performed by selecting dominant principal components (PCs) that contain most of the clinical information. L.N. Sharma et al. [16] utilized the PCA decomposition on various WT coefficients that reduced all correlations between them. The same authors [17] proposed Daubechies WT up to 6^{th} level, for multi scale PCA decomposition of 2D ECG data. S. Padhy et al. [18] introduced a new approach of 3D tensor representation of 2D MECG data and used higher order SVD (HOSVD) for tensor decomposition, followed by data reduction. An improved result of their work [19], by utilizing multiscale HOSVD, provided a great result. They achieved maximum CR of 45 along with minimum PRD of value 2.71. Though in some records, after reconstruction, PRD was higher than 25%, as mentioned in their paper. Therefore, quality aware [21] compression of MECG data is very necessary to control the PRD within a specified value. Quality controlled compression [22] assures this fact that after reconstruction, clinical features would not get destroyed as well as keeping high CR. In recent works [23], beat-wise dimension reduction using PCA along with quality aware compression based on PSO, provided satisfactory result of CR of value 16.2 and PRD of 1.47.

The ECG characteristic depends on patient's age, gender, physical condition, heart diseases etc. Thus while evaluating ECG, all these personal information of patient should be available to the doctor [25]. But according to Health Insurance Portability and Accountability Act (HIPAA) of 1996, patient's personal information should not be disclosed and patient privacy should be maintained and secured from cyber-attacks. Hence, not only compression, data concealing is also necessary [26]. ECG steganography is an efficient approach of hiding (encrypting) patient's personal data within respective ECG signal in a proper approach that these data should not be detected by naked eyes, except intended personnel, who can decrypt those information by reverse algorithm of data insertion. Very few papers [27,28] have been published on both single lead data compression and steganography and that too mainly based on WT, SVD. To the best of authors' knowledge, till now, there is no published work on MECG data compression and steganography. In addition. 3D tensor decomposition based MECG data compression was performed in very few published works, [18–20], using fixed quantization level to quantize the compressed data which resulted in high PRD in some leads [19]. Also while constructing the 3D beat tensor, dimension of that tensor was made fixed (10 successive beats) in the previous works, thus the variation of result was not compared using more or less beats to create beat tensor.

In this work, to reduce all types of redundancies, tensor decomposition based MECG data compression was proposed using Tucker deposition (TD) algorithm. To reduce the computational complications and execution time, 2-mode PCA based TD was first introduced in this work. To conceal patient's information by maintaining data privacy, steganography was performed, within least significant PCs of reduced beat tensor, followed by generation of 'secret key'. This 'secret key' ensured that only the intended personnel would be able to get the information about the personal data of respective patient after decompression. To make sure about least distortion of MECG after reconstruction as well as enhancement of CR, i.e. to improve the quality of compression, an offline trained multi-agent supervised learning system (MASLS) was first proposed to allocate optimal quantization level to each fiber of beat tensor. The ANN was trained using features of PCs and previously optimized data of those PCs from PSO, so that the PRD could be limited within 5% resulting in high CR. A feature refers to distinguishable [29] characteristics of PC and classification of those features [30] was necessary for training the ANN. During reconstruction (using reverse algorithm of compression), user must provide correct 'secret key', that was generated during compression, to know the patient's confidential information along with MECG data, failing which, only data reconstruction would be done. Thus the main contributions of this work are, 1) MECG data compression on 3D beat tensor (constructed using 5, 10 and 15 successive beats, separately) using Tucker decomposition (TD), 2) introduction of 2-mode PCA decomposition based on TD, 3) implementation of steganography of MECG data compression, and 4) quality controlled compression using PSO and MASLS ensuring minimum reconstruction error. The rest of this paper is organized as follows; Section 2 explains the methodology used in this work, Section 3 shows obtained result; Section 4 compares this result with previously published works and finally Section 5 concludes this paper.

2. Method

Fig.1 shows the signal processing flow diagram of this proposed work. Data compression process was initiated by selecting 8 independent leads, which were first de-noised to filter out the high frequency information. After R-peak detection and beat extraction, 3D beat tensor was formed using MECG data, on which, PCA based Tucker decomposition was implemented to reduce the interbeat and interlead redundancies. To conceal patient's information, steganography was performed within the least significant PCs of reduced beat tensor. To limit the PRD within specified value, PSO and MASLS were used to allocate optimal quantization level to each PC of beat tensor. Intrabeat redundancy reduction was performed using double delta encoding and run length encoding, which also increased the CR sufficiently. Finally, after header byte creation, the compressed data was stored.

2.1. Preprocessing and 2D beat matrix formation

Owing to internal dependency of 12 leads, only 8 leads (I, II, V1, V2, V3, V4, V5 and V6) were selected, because rest of the leads (III, aVR, aVL, aVF) can be computed using following equations [31],

$$\begin{aligned} \mathrm{III} &= \mathrm{II} - \mathrm{I} \\ \mathrm{aVR} &= -0.5 \times (\mathrm{I} + \mathrm{II}) \\ \mathrm{aVL} &= 0.5 \times (\mathrm{I} - \mathrm{III}) \\ \mathrm{aVF} &= 0.5 \times (\mathrm{II} + \mathrm{III}) \end{aligned} \tag{1}$$

Due to the presence of high frequency noise, each selected lead was first de-noised using a low pass 4^{th} order Butterworth filter of 100 Hz cut off frequency, because most of the clinical information are present within this frequency range. Then R-peaks were detected using derivative based approach, which is a time saving algorithm of peak detection with less computational complexity. Now after detection of each peak, onset and offset of corresponding beat was calculated using the following equations,

$$\begin{aligned} R(l)_{onset} &= R(l) - 0.33 \times (RR_{l-1,l}) \\ R(l)_{offset} &= R(l) + 0.67 \times (RR_{l,l+1}) \end{aligned} \tag{2}$$

where $R(l)_{onset}$, $R(l)_{offset}$ are the onset and offset position (here position refers to sample index) of l-th R-peak position $R(l)$, respectively and $RR_{l1,l2}$ represents the RR interval between $l1$ and $l2$-th R-peak [32]. With the help of these positions, using 'p' number of successive beats from each lead, a 2D beat matrix was formed by aligning all R-peaks in same position with normalized beat length of sample number 'q', by last sample padding. In this way, for 8 leads, 8 beat matrices were formed of order ($p \times q$). This 2D representation was updated to 3D tensor representation, for further computation.

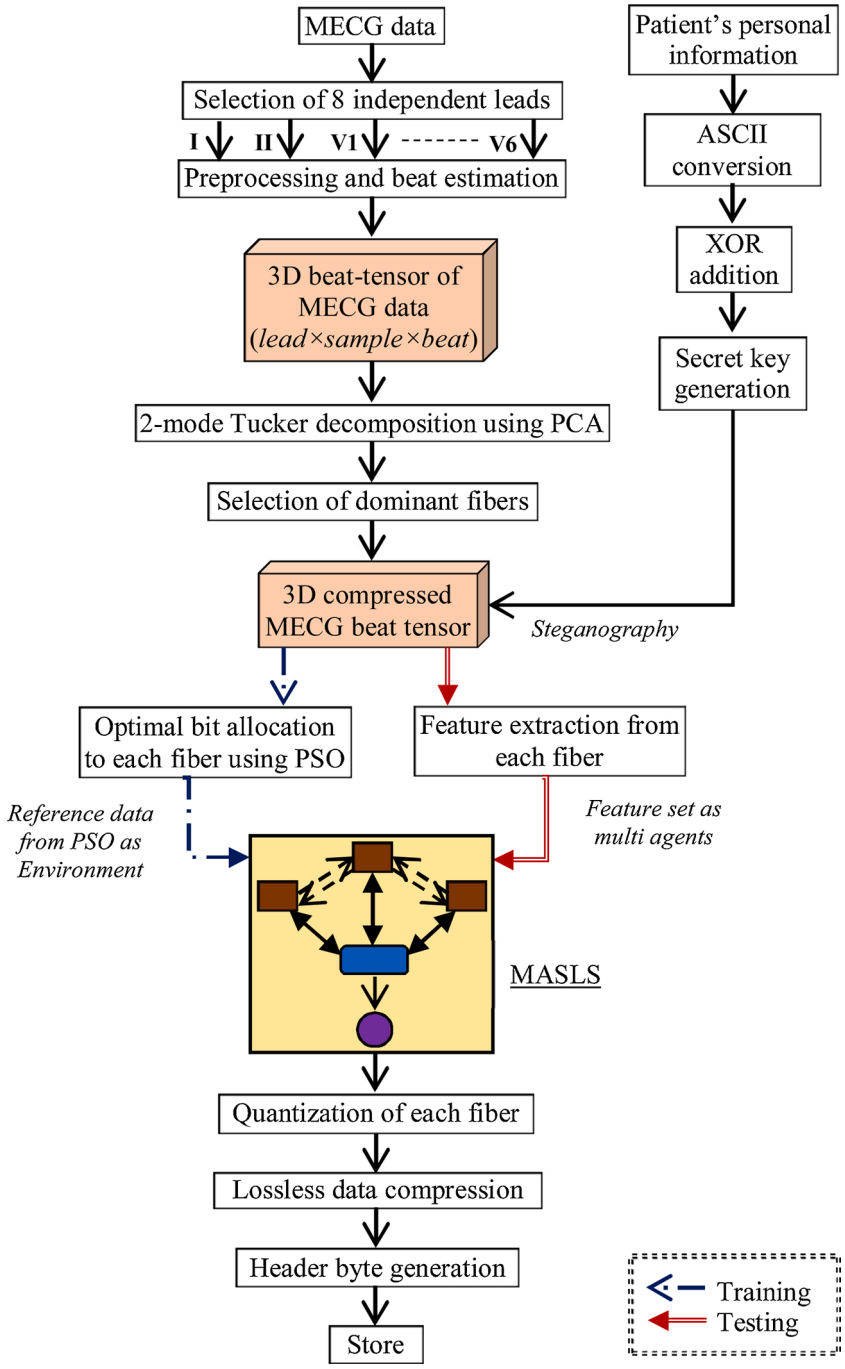

Fig. 1. Signal processing flow diagram of proposed work.

2.2. Concept of tensor and Tucker Decomposition (TD)

A tensor [33] of order N is denoted as $\mathscr{B} \in \mathbb{R}^{I_1, I_2 \ldots I_N}$ where each element of this tensor is $b_{i_1, i_2 \ldots i_N}$. A 3D tensor can be denoted by $\mathscr{X} \in \mathbb{R}^{m \times n \times l}$ with elements denoted as $\mathbf{x}_{i,j,k}$ where $i = 1,2\ldots\ m$; $j = 1,2..n$; $k = 1,2..l$. Hence, a tensor $X^{m \times n}$ is of order 2 i.e. $X \in \mathbb{R}^{m \times n}$, is basically a 2D matrix with number of rows and columns of number 'm' and 'n', respectively. A '*fiber*' of a tensor is a one dimensional matrix along each dimension i.e. for 3D tensor, mode-1 fiber is tube vector expressed as $X_{:,j,k}$. Similarly, mode-2 and mode-3 fiber are row and column vectors, expressed as, $X_{i,:,k}$, $X_{i,j,:}$, respectively. A '*slice*' refers to 2D section of tensor, which is basically a 2D matrix, expressed as $X_{i,:,:}$, $X_{:,j,:}$,$X_{:,:,k}$ that are named as horizontal, lateral and frontal slice, respectively.

The Tucker decomposition (TD) [34] (introduced by Tucker in 1963) is a form of higher order PCA, generally used for data compression. In this process, the mother tensor $\mathscr{X}$ is decomposed into a core tensor $\mathscr{G}$, multiplied by one matrix along each mode. For a 3D tensor, this decomposition is performed by the following equation,

$$\mathscr{X} \approx \mathscr{G} \times {}_1A^{(1)} \times {}_2A^{(2)} \times {}_3A^{(3)} \approx [\![\mathscr{G} :]\!]_1 A^{(1)}, {}_2A^{(2)}, {}_3A^{(3)} \tag{3}$$

where each element can be expressed as,

$$x_{i,j,k} = \sum_{i=1}^{m'} \sum_{j=1}^{n'} \sum_{k=1}^{l'} g_{ijk} a_i^{(1)} \circ a_j^{(2)} \circ a_k^{(3)} \tag{4}$$

where ${}_1A^{(1)} \in \mathbb{R}^{m \times m'}$, ${}_2A^{(2)} \in \mathbb{R}^{n \times n'}$, ${}_3A^{(3)} \in \mathbb{R}^{l \times l'}$ are the 2D factor matrices, which are likely to be orthogonal, and they represent two

dimensional decomposition along three modes. The tensor $\mathscr{G} \in \mathbb{R}^{m' \times n' \times l'}$ is named as core tensor, where *m', n', l'* are the number of elements along X, Y, Z-axis. Now, if $m' < m$, $n' < n$, $l' < l$, then it can be concluded that the mother tensor $\mathscr{X}$ is compressed to the core tensor $\mathscr{G}$; which ensures data reduction [35]. The operator '$A \circ B$' represents the vector outer product between '*A*' and '*B*'. This process is shown in Fig. 2. In this work, '2-mode Tucker decomposition' along with compression was introduced by decomposing the mother tensor along two modes among three modes of decomposition.

2.3. 2-mode TD using PCA on 3D beat tensor

On the basis of the concept of 3D tensor, using the 2D beat matrices of MECG data, a 3D beat tensor, $\mathfrak{T} \in \mathbb{R}^{p \times q \times r}$, of order $(p \times q \times r)$ can be formed [36], where *p, q, r* represent the number of beats, number of samples in each beat and number of leads, respectively. A clear visualization of this tensor is shown in Fig. 3(a), where each frontal slice of order $(r \times q)$ represents the beat matrix, by aligning R-peaks of each single beat from all leads ('*r*'), in same position; the horizontal slices are 2D matrices of order $(p \times q)$, formed using all beats ('*p*') form each single lead, by padding the last samples of every beat to make the length of each beat equal to '*q*' [37]. Now, implementation of PCA needs a 2D array or matrix [38]; hence 'Matricization' of beat tensor is necessary.

The 'Matricization', also known as 'unfolding' of tensor [39], is a process of transforming a tensor into matrix. A mode-n unfolding of tensor $\mathscr{B}$ is represented by $B_{(n)}$, by aligning mode-n fibers of $\mathscr{B}$ sequentially, so that it forms each column of $B_{(n)}$; e.g. a tensor of order $(3 \times 4 \times 5)$ can be represented as 2D matrices in three different ways of order (3×20), (5×12) or (4×15). In this work, the beat tensor $\mathfrak{T}$ was first decomposed into mode-p frontal slices expressed as $X_{(p)}$

$$\mathfrak{T} \approx X_{(1)}, X_{(2)}, \ldots X_{(p)} \text{ where} X \in \mathbb{R}^{r \times q} \tag{5}$$

where the elements of *i*-th slice, $x_{k_{(i)} j_{(i)}}$ can be viewed as

$$x_k(i)_{,j}(i) = \mathfrak{T}_{i,j,k}, \tag{6}$$

where $i = 1,2,\ldots p$; $j = 1,2,\ldots q$; $k = 1,2,\ldots r$. Now, finally the 2D matricization of mode-p was performed using following equation,

$$A = \sum_{i=1}^{p} (X_{(i)} \otimes \mathbb{C}_i^m) \tag{7}$$

where '*Z*' and '*I*' are zero and identity matrix respectively and $\mathbb{C}_i^m = \left[Z^{1,(i-1)} I^{1,1} Z^{1,(m-i)}\right]$ (e.g. for $i = 2$ and $m = 4$, the $\mathbb{C}_2^4 = [0\ 1\ 0\ 0]$). The operator '$A \otimes B$' represents the Kronecker product between '*A*' and '*B*'. In this way, the beat tensor was transformed into equivalent matrix '*A*' such as, $\mathfrak{T} \approx A \in \mathbb{R}^{r \times m}$ where $m = (p \times q)$ and each element is represented as,

$$A_{i_1 j_1} = \mathfrak{T}_{i,j,k}$$

$$i_1 = (r - k + 1); j_1 = [\{(p - i) \times q\} + j] \tag{8}$$

where $i_1 = 1, 2 \ldots r$ and $j_1 = 1, 2 \ldots m$. Now, PCA was performed on this matrix by computing the mean matrix $AM \in \mathbb{R}^{1 \times m}$ and mean subtracted matrix $\overline{A}$ as followed,

$$AM_{1,m} = \frac{\sum_{u=1}^{r} A_{u,m}}{r}$$

$$\overline{A_{i_1 j}} 1 = A_{i_1 j} 1 - AM_{1,j} 1 \tag{9}$$

Finally, the eigen value - eigen vector decomposition of a symmetric matrix $\varphi 1 \in \mathbb{R}^{r \times r}$ was computed as,

$$\varphi 1 = [\overline{A} \times \overline{A}^T]$$

$$\varphi 1 \times \nu = \lambda \times \nu$$

$$\varepsilon 1 = \nu^T \times \overline{A} \tag{10}$$

where $\nu \in \mathbb{R}^{r \times r}$ is eigen vector matrix and $\lambda \in \mathbb{R}^{r \times r}$ is a diagonal matrix. The principal component matrix $\varepsilon 1 \in \mathbb{R}^{r \times m}$ was arranged in decreasing order of variance. Now, the selection of dominant PCs or rows, was performed using energy restoration efficiency (ERE) criteria computed upon diagonal elements of λ i.e. $\lambda_{\widehat{i}} = diag(\lambda_{\widehat{i},\widehat{i}})$ where $\widehat{i} = 1, 2 \ldots r$ as,

$$E_{r'} = \frac{\sum_{i=1}^{r'} \left(\lambda_{\widehat{i}}\right)^2}{\sum_{j=1}^{r} \left(\lambda_{\widehat{j}}\right)^2} \geq 0.99 \tag{11}$$

The above equation provided the value of '*r*'' for which $E_{r'} \geq 99\%$. Thus after selection of *r'* dominant PCs, the matrix was converted to $\varepsilon 1' \in \mathbb{R}^{r' \times m}$ where $r' < r$. Finally, this matrix $\varphi 1$ was transformed back to 3D tensor, $\mathfrak{T}' \in \mathbb{R}^{p \times q \times r'}$, with reduced horizontal slices from *r* to *r'* in such a way that each element of this tensor is represented as,

$$\mathfrak{T}'_{i,j,k'} = \varepsilon 1'_{g_1, h_1} \tag{12}$$

where, $g_1 = (r' - k' - 1)$; $h_1 = [\{(p - i) \times p\} + j]$; and $k' = 1, 2..r'$. In this way 1-mode compression of 3D beat tensor was performed. The 2-mode compression using PCA was initiated by transforming the new beat tensor $\mathfrak{T}'$ again into another 2D matrix *B*, such as $B \in \mathbb{R}^{p \times n}$ where$n = (r' \times q)$; using horizontal slices $Y_{(r')}$, such as $\mathfrak{T}' \approx Y_{(1)}, Y_{(2)}, \ldots Y_{(r')}$, where $Y \in \mathbb{R}^{p \times q}$ and each element of *k'*-th slice is denoted as $y_i(k')_{,j}(k') = \mathfrak{T}'_{i,j,k'}$. Thus, *B* was formed as followed

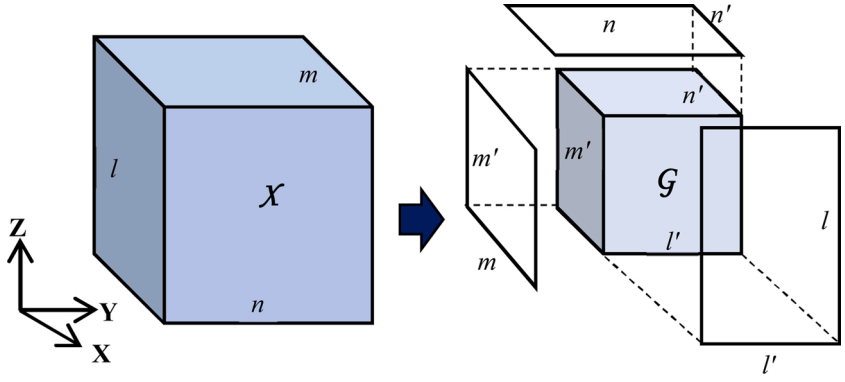

Fig. 2. 3D-mode Tucker decomposition of 3D tensor.

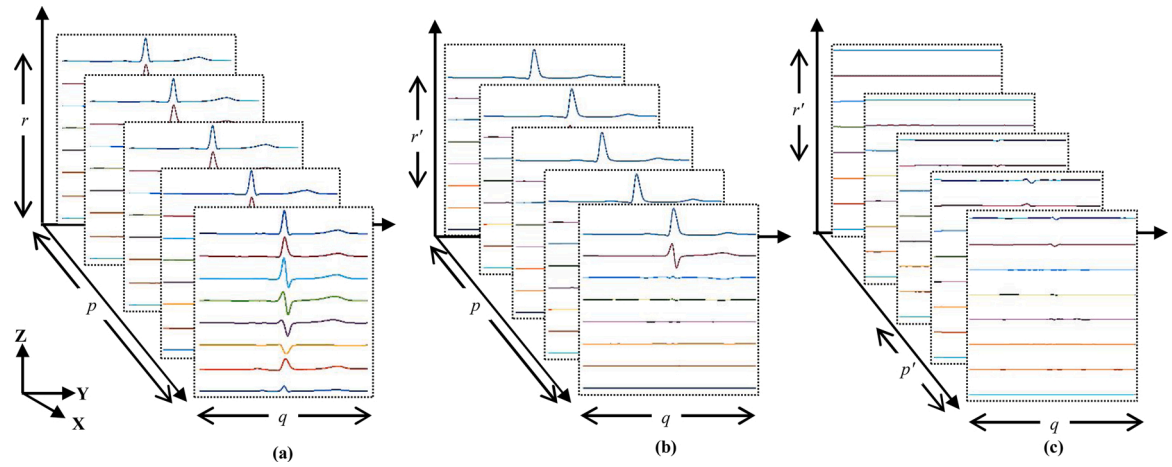

Fig. 3. 2D PCA decomposition on 3D beat tensor, (a) 3D representation of original beat tensor, (b) mode-1 decomposition along Z-axis, (c) mode-2 decomposition along X axis.

$$B = \sum_{k'=1}^{r'} (\mathrm{Y}_{(k')} \otimes \mathbb{C}_{k'}^{n}) \tag{13}$$

Each element of B is denoted as $B_{i_2,j_2} = \mathfrak{T}'_{i,j,k'}$ where, $i_2 = i$, $j_2 = [\{(r' - k') \times q\} + j]$, $i_2 = 1, 2...p$ and $j_2 = 1, 2...n$ aligned sequentially to form each column fiber of B. Now, PCA decomposition on B was performed by following equations, in a similar way mentioned earlier,

$$BM_{1,n} = \frac{\sum_{w=1}^{p} B_{w,n}}{p}$$

$$\overline{B_{i_2,j_2}} = B_{i_2,j_2} - BM_{1,j_2}$$

$$\varphi 2 = [\overline{B} \times \overline{B}^{T}]$$

$$\varphi 2 \times \nu' = \lambda' \times \nu'$$

$$\varepsilon 2 = \nu'^{T} \times \overline{B} \tag{14}$$

where $BM \in \mathbb{R}^{1\times n}$ is mean matrix and $\overline{B}$ is mean subtracted matrix of B; $\varphi 2 \in \mathbb{R}^{p\times p}$; $\nu' \in \mathbb{R}^{p\times p}$ and $\lambda' \in \mathbb{R}^{p\times p}$ are eigen vector and eigen values respectively and $\varepsilon 2 \in \mathbb{R}^{p\times n}$ is the principal component matrix in 2nd mode PCA decomposition. As performed earlier, selection of dominant PCs was performed by ERE criterion using diagonal elements of λ' as,

$$E_{p'} = \frac{\sum_{h=1}^{p'} (\widehat{\lambda'_h})^2}{\sum_{k=1}^{p} (\widehat{\lambda'_k})^2} \geq 0.90 \tag{15}$$

The above equation provided the value of 'p'' for which $E_{p'} \geq 90\%$. Thus after selection of p' dominant PCs, the matrix was converted to $\varepsilon 2 \in \mathbb{R}^{p'\times n}$ where $p' < p$. Finally, this matrix $\varphi 2$ was again transformed back to 3D tensor, $\mathfrak{T}'' \in \mathbb{R}^{p'\times q\times r'}$, with reduced frontal slices from p to p' in such a ways that each element of this tensor is represented as,

$$\mathfrak{T}''_{i',j,k'} = \varepsilon 2'_{g_2,h_2} \tag{16}$$

where $g_2 = p'$; $h_2 = [\{(r' - k') \times q\} + j]$; $i' = 1, 2..p'$ and $\mathfrak{T}'' \in \mathbb{R}^{p'\times q\times r'}$. Thus after performing 2D PCA decomposition and compression, the mother beat tensor $\mathfrak{T} \in \mathbb{R}^{p\times q\times r}$ was finally reduced to $\mathfrak{T}'' \in \mathbb{R}^{p'\times q\times r'}$ viz. reduction of total elements was done from $(p \times q \times r)$ to $(p' \times q \times r')$ where, $p'<p$, $r'<r$.

This 2D compression using PCA is similar to 2-mode Tucker decomposition (TD), in which the core tensor of TD is equivalent to finally compressed tensor $\mathfrak{T}''$ and the two 2D matrices in TD are equivalent to two eigen vectors, obtained from PCA in mode-1 and mode-2, i.e. $\nu^{r\times r}, \nu'^{p\times p}$.

2.4. Optimal quantization using PSO

Quantization of compressed data is an important part of compression process for storing or transmitting in remote tele-monitoring system. Manual provision of quantization bit (Q_{bit}) results in higher CR and higher PRD for lower Q_{bit} and vice-versa. Now, each row fiber of the core tensor $\mathfrak{T}''$ represents each PC with monotonically decreasing order of variance, along both Z and X-axis (refers to Fig. 3). These PCs contain clinical information, which varies based on their variance viz. PC with highest variance possesses most information and vice-versa. Keeping this fact in consideration, while quantizing these PCs, fixed quantization to all of them is not justified. Hence, optimal quantization level was provided by an offline trained PSO [40], to limit PRD within 5%. In general, PSO searches for optimal best solution, arbitrarily [41,42] within the specified search space. The main disadvantage of this procedure is, sometime PSO provided comparatively low Q_{bit} for higher energy PCs and higher Q_{bit} for lower energy PCs. Now, as in the $\mathfrak{T}''$ tensor, number of higher energy PCs, is comparatively lesser than lower energy ones; hence in such search result, though the overall PRD might be less than 5%, the CR would be lower. But, higher CR and lower PRD is always desired. For this reason, PSO was implemented in such a way that, PC with higher energy (or variance) would be assigned by higher Q_{bit} and PC with lower energy, would get lower Q_{bit}. Using this criteria, the search space of Q_{bit} was kept in between [4,10] and the PSO was used to find out the optimal quantization level for each horizontal fiber of tensor $\mathfrak{T}''$ so that the overall PRD was limited between 5% as well as quality of ECG would be maintained. The cost function of PSO, $f(\bullet)$ was assumed as,

$$\min_{c\in D}, f_n(c), \text{subject to} |prd_c \sim prd_d| \approx 0.05 \tag{17}$$

where 'c' is the quantization level computed by PSO within the search space D, 'prd_c' is overall PRD computed by the PSO in each iteration i.e. candidate solution, and 'prd_d' is the desired PRD i.e. 5%. The PSO was so performed that it will provide lowest Q_{bit} to $\mathfrak{T}''_{1,:,1}$ fiber and highest Q_{bit} to $\mathfrak{T}''_{p',:,r'}$ fiber shown in Fig. 3(c).

The position and velocitie of each particle were updated in each iteration using the following equation,

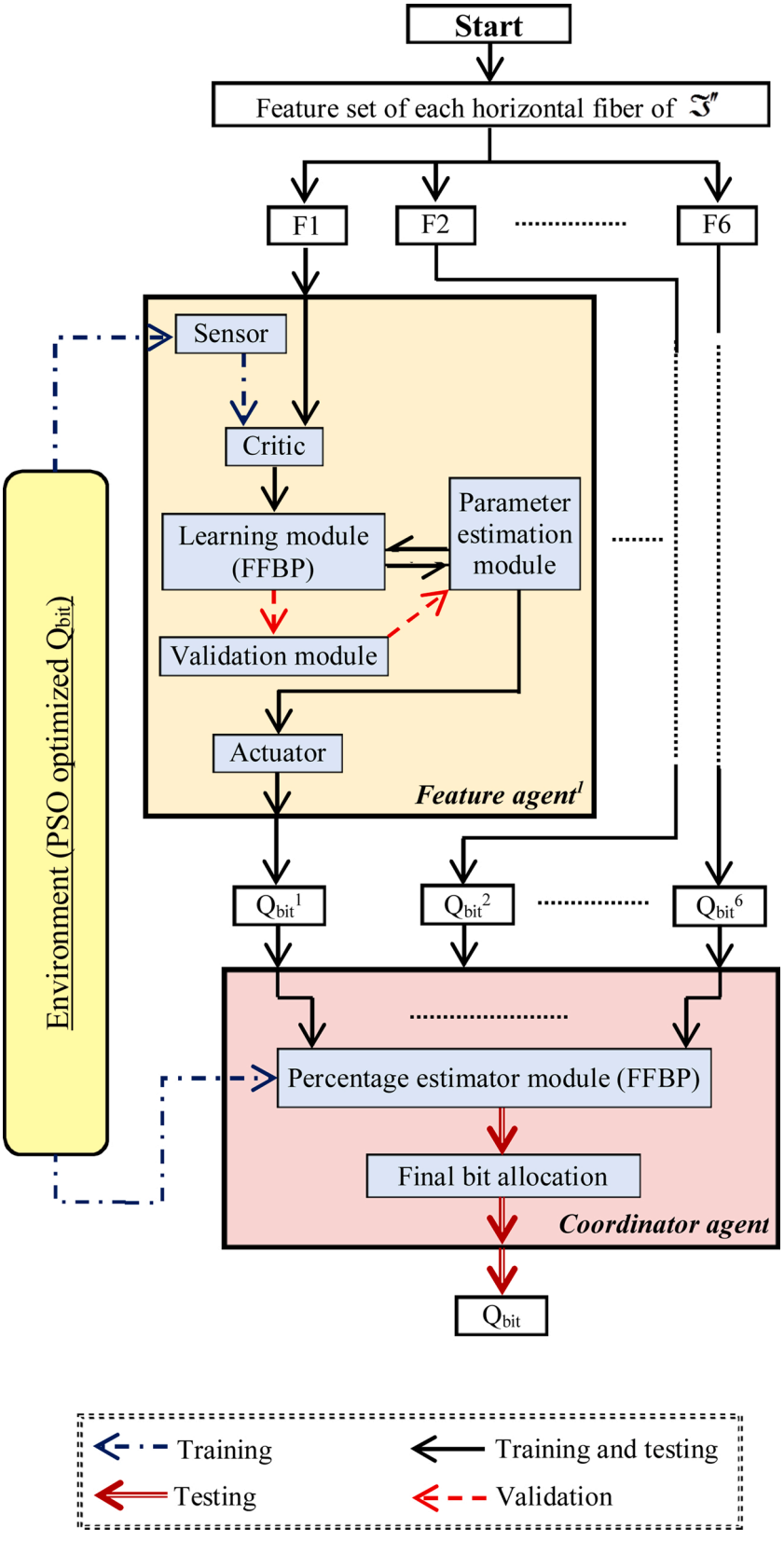

Fig. 4. Signal processing flow diagram of MASLS.

$$y_{k+1}^{i} = y_k^i + v_{k+1}^i$$
$$v_{k+1}^{i} = v_k^i + c_1 r_1 \left(p_k^i - y_k^i\right) + c_2 r_2 \left(p_k^g - y_k^g\right) \quad (18)$$

where, y_k^i : each particle position; v_k^i : each particle velocity; p_k^i : best position remembered by each particle (p_{best}); p_k^g : best position remembered by swarm (g_{best}); c_1, c_2: cognitive and social parameters; r_1, r_2 : random variables between 0 and 1.

In this way, quality of ECG was maintained by keeping the most significant PCs almost unaffected by providing them higher quantization level; in addition the CR was increased by providing lower Q_{bit} for less significant fibers.

2.5. Multi Agent Supervised Learning System (MASLS)

PSO, being a time consuming process, could not be used for optimal bit allocation, in each case. Therefore, an offline trained artificial neural network (ANN) was used for this purpose, using the PSO generated information, as reference. A set of 150 input-output dataset were used for ANN training and validation. The input set was formed, using six features of each horizontal fiber or PC of final reduced tensor i.e. $\mathfrak{T}''$, to train the network, so that it would provide optimal Q_{bit}, which was the output data set of PSO. Implementation of deep learning [43,44] to classify the features might improve the result, but it also enhanced the execution time as feature extraction was performed for each record while compression. A feature refers to distinguishable characteristics of each PC which were selected as, 1) percentage of energy of corresponding eigen vector (F1), 2) average energy of fiber or PC (F2), 3) average slope energy of PC (F3), 4) min-deviation (F4), 5) max-deviation (F5) and 6) max-min bandwidth (F6), (it was observed that variation of these features was distinguishable depending upon the quantization levels, optimized by the PSO) of each PC. Now as they were independent features, training and testing using them assuming 'multiagents' would provide better result than as a 'single agent'[45]. In multiagent system, each and every agent can learn through same *environment* independently to achieve *agent goal*, through proper learning algorithm. The general structure of a learning agent is mentioned in [46], where an *agent* refers to any object that perceives or realizes the input response from the external world called *environment* and also can act upon the *environment* through *actuator*, using mathematical formulation called *agent function*. In the *learning agent* architecture [46], authors proposed four different modules viz. 1) *learning element*, which utilizes the feedback from *critic* to make further improvements to the system, 2) the *critic* element, which makes the learning element knowledgeable about the growth of its improvement using the *environment* through *sensor*, 3) *performance element*, that takes necessary actions to make improvements based on agent inputs, and finally 4) *performance generator* provides the suggestive actions that are necessary for new and informative events. There are mainly three types of machine learning approaches viz., 1) supervised learning, where critic provides actual behavior of the agent, for any given situation, 2) unsupervised learning, which is basically an aimless learning i.e. critic cannot provide sufficient information so that the system can improve its behavior, and 3) reinforcement learning, in which, the system improves its behavior using some given task by the environment based on given rewards [47].

In this work, the critic can provide correct response i.e. PSO optimized Q_{bit}, to the system; that ensures supervised learning in multiagent system (MAS). Therefore, each feature (F1, F2,…F6) was assigned as '*feature agent*'s, which were trained in decentralized mode i.e. each agent was trained independently. Another agent called '*coordinator agent*' was also used, that was trained using the output of each *feature agent* to provide final Q_{bit} at testing period. This algorithm is shown in Fig. 4. The MASLS procedure is explained below.

2.5.1. Training-1

Each feature agent contained a learning module, which utilized feed forward back propagation (FFBP) approach. Being a supervised learning, the 'critic' provided the actual output or optimized Q_{bit} through 'sensor' of the module, from the 'environment', along with the respective feature, at training period. The learning module continued adjusting its weights using the parameter estimation module. The learning module performed the improvement for adjacent weight matrices, which were updated within' parameter estimation module'. This training was performed using 1000 epochs and 3 hidden layers with 30 neurons in each (the parameters of ANN were so chosen that minimum validation error occurs along with low convergence time of training), using gradient descent with momentum (GDM) backpropagation (BP) algorithm.

2.5.2. Validation

Now the accuracy of Training-1 was measured and improved using 10-fold, cross validation, which was performed using validation module, and final weight adjustment was performed using 'parameter estimation module'. For validation, entire dataset was divided into 10 subset, containing 15 dataset in each. Thus, the ANN was trained 10 times and after completion of each training process, maximum absolute error (MAE) was computed. Finally, this error of training was 2.14% in average. As it was a supervised learning, the actuator neither provided any output or agent action to the environment nor any reward was send back to the agent. Hence, after completion of training and validation, each feature agent was able to provide quantization level, separately.

2.5.3. Training-2

Now, for same PC, all *feature agents* might not provide same quantization level (e.g.Q_{bit}^1, Q_{bit}^2. Q_{bit}^6 as mentioned in Fig. 4, might not be same) during validation period; but, it should be equal to PSO optimized final Q_{bit}, for all. Therefore, the 'coordinator agent' utilized *cooperative learning* to meet the same *goal* i.e. PSO optimized Q_{bit}. This agent took the output of each *feature agent* as input dataset and the *percentage estimator module* within this agent, assigned corresponding 'percentage of acceptance (***PA***)' for each *feature agent* output, to provide final optimized quantization level.

2.5.4. Testing

After completion of training and validation, testing was done using 12241 data (including entire training data). Among them, total 200 data (including 50 training data) were used for finding the accuracy of finally trained network in form of MAE, which was 1.77%. During testing period, the 'environment' became idle in operation i.e. 'critic' provided features of each single PC to 'learning module' for each feature agent. Using the estimated weight matrix, 'parameter estimation module' provided the quantization level. Thus, six separate values (outputs of feature agents) of quantization level for single PC were fed into the coordinator agent. The coordinator agent then provided ***PA*** to each Q_{bit}^t, to calculate the final quantization level of that PC, provided by MASLS using following equation,

$$Q_{bit}^{NN} = \frac{\sum_{t=0}^{6}\left(Q_{bit}^t \times P^t\right)}{100}$$
$$\sum_{t=0}^{6} P^t = 100 \quad (19)$$

where Q_{bit}^t and P^t is the quantization level provided by t-th feature agent and the percentage of acceptance (***PA***) to Q_{bit}^t provided by the coordinator agent, respectively. Q_{bit}^{NN} is the final quantization (rounded off to nearest integer) level allotted to respective PC, computed by MASLS. In this way, using the optimized output of PSO, the MASLS was used to provide optimal quantization level to each PC, to limit the overall PRD within 5%, which ensured quality controlled compression.

2.6. Steganography procedure

After quantization, delta encoding was applied on quantized PCs. Delta encoding is a lossless procedure that computes the difference between successive samples. In this work, at first, delta encoding was implemented on quantized PCs twice, as a lossless encoder. Data concealing was performed on delta encoded array, after generating a 'secret key' [48] containing five elements as [**K1 K2 K3 K4 K5**]. To encrypt patient's confidential information, at first patient's confidential data were converted to equivalent ASCII code of each character, followed by elementary XOR addition with binary equivalent of first element of secret key i.e. **K1**. Now, it can be observed in the reduced beat tensor, those fibers nearer to origin i.e. (0, 0, 0) viz. $\mathfrak{F}''_{1,:,1}$, $\mathfrak{F}''_{1,:,2}$, $\mathfrak{F}''_{2,:,1}$ and $\mathfrak{F}''_{2,:,2}$ contain least energy, as shown in Fig. 3(c). Therefore, steganography was performed by replacing 'N_{bit}' number of samples from both end of these four fibers, of 'N_{tns}' number of corresponding tensors, sequentially, with secret bit-stream. The rest four elements of 'secret key' generated as; **K2**= 'N_{bit}', **K3**='N_{tns}', **K4**= last modified fiber of 'N_{tns}-th tensor and **K5**=number of sample replaced from **K4**-th fiber. The following example can provide an easier realization: if 1083 bits are intended to hide with **K2** = 50 (i.e. from each fiber mentioned above, 50 number of samples from each end, are to be replaced by secret bits, sequentially), which means, maximum ($50 \times 4 \times 2$=) 400 bits can be hidden in each successive tensor. Thus after concealing 800 bits within two tensor, (1083-800=) 283 bits are needed to be replaced in 3rd tensor; hence **K3** will be 3. Now, in the 3rd tensor, among 283 bits, total 200 bits can be stored in first two fibers i.e. $\mathfrak{F}''_{1,:,1}$, $\mathfrak{F}''_{1,:,2}$ and rest (283-200=) 83 bits are needed to be stored in 3rd fiber i.e. $\mathfrak{F}''_{2,:,1}$; hence, **K4** will be 3 and **K5** should be 83 (for convention, first 50 bits would be replaced from P-wave end of corresponding fiber and the rest 33 bits would be stored from T-wave end). In this way, after provision of value **K1** and **K2,** the value of **K3**, **K4** and **K5** were generated by algorithm and finally, the 'secret key' would be available to user which was needed during decompression only if secret data decryption was necessary.

In this way, a secret key was generated separately from the compressed MECG data. While reconstruction, if user wished to decrypt those hidden information, the same secret key was necessary otherwise, only MECG data would be reconstructed.

2.7. Lossless coding and data store

To reduce intrabeat redundancy, run length encoding was used on the delta encoded array, resulting in increasing CR sufficiently without effecting PRD. All eigen vectors along with extrema of each PC, were quantized with fixed quantization level (8 bit). Finally, entire compressed data were stored after formation of header byte, which refers to allocation of fixed number of bytes to store necessary information that were useful to reconstruct MECG data. The structure of header byte is shown in Table 1.

3. Result

This algorithm was implemented on 12-lead ECG database available on ptbdb [49]. In this database, total 549 MECG records are present which are categorized among nine types of annotation or heart disease viz. Myocardial infarction, Bundle branch block, Myocarditis, Cardiomyopathy/Heart failure, Myocardial hypertrophy, vulvar heart disease, Healthy control and Miscellaneous. Among them, total number of 377, 17, 4, 18, 7, 6, 72 and 29 records from the mentioned annotation types were used, respectively. These signals are recorded from 290 patients aged between 17 and 87 with mean value 57.2. Amongst them, 81 patients were female and 209 were male with mean age of 61.6 and 55.5, respectively (age of 1 female and 14 male patients were not recorded). Each signal was digitalized in 1 kHz sampling frequency with 16 bit data resolution. Every record includes 15 simultaneously measured signals including 12 leads (I, II, III, aVR, aVL, aVF, V1, V2, V3, V4, V5 and V6) and 3 Frank lead ECGs (Vx, Vy, Vz). In this work, only 12 conventional leads were used for computation. As the compression procedure initiated by the formation of beat tensor, accurate R-peak detection was mandatory which was performed using derivative based approach on lead V6 of each MECG signal. The overall accuracy was achieved 98.95%. Finally, the beat tensor was formed using 8 independent leads. The result of compression was measured using CR, PRD and PRDN [50]. For each MECG record, observation of compression result was performed by creating three different beat tensor viz. 5, 10 and 15- beat tensor using 5, 10 and 15 successive beats, respectively. In this section, for the sake of understanding, each compression result is mentioned, indicating the respective tensor-beats under subscript within third bracket e.g. a CR of value $22_{[10]}$ implies that a CR of 22 is measured for 10-beat tensor. Table 2 describes the obtained result with all cardiac abnormalities, for 5, 10 and 15-beat tensor. Along with overall CR, PRD and PRDN, lead wise PRD variation is also shown in this table. After testing on 547 records, average CR of $22_{[5]}$, $41.5_{[10]}$, $55.4_{[15]}$, PRD of $3.62_{[5]}$, $4.96_{[10]}$, $5.59_{[15]}$ and PRDN of $3.61_{[5]}$, $4.94_{[10]}$, $5.57_{[15]}$ was achieved for 5, 10, 15-beat tensor, respectively. Fig. 5 shows a segment of original and reconstructed signals of ptbdb data id: 273s0511_re ('Myocardial Infarction') for 10 beat tensor decomposition. This whole algorithm was implemented on system configuration of Intel i5 CPU, 3.19 GHz processor, in MATLAB/Simulink.

Table 1
Header Byte Structure.

Sl. No.	Description	No. of allocated bits
1	Number of beat tensor (N_b)	2
2	Number of PCs (N_p)	5
3	Extrema of PCs and eigen vectors	{(4)+(4 × 2)}×8
4	Quantization levels	3× N_p
5	Quantized eigen vector	{(8 × 8)+(N_b × N_b)}×8
6	Quantized and encoded PCs	-

4. Discussion

Table 3 describes a comparative study of proposed method with recently published works on MECG data compression. A. Cetin et al. [11] introduced various transform domain coding techniques viz. DCT, KLT, on MECG data to transform it into frequency domain coefficients. The higher energy coefficients were coded using subband coder and lower energy coefficients were coded using multirate transform coder. Authors achieved PRD of 6.19 along with CR 6.17 using DCT and 7.98 using KLT, separately. An advancement of MECG data compression was further shown using DWT in [12]. Authors stored only the residue of highly correlated wavelet coefficients to achieve high CR of 18, but on the other hand it enhanced the PRD up to 11. To reduce this error, J. Wei et al. implemented SVD upon MECG data to reduce the correlation, present within it followed by storing the higher energy coefficients. CR and PRD were achieved of value 10 and 1.18 in their work. An improvement of WT was reflected in [17] using PCA. Authors utilized PCA on various wavelet coefficients and achieved CR and PRD of 5.98 and 2.09, respectively. S. Padhy et al. [18] first introduced 3D beat tensor terminology, while compressing MECG data using 10 successive beats. They implemented WT and HOSVD that readily increased the CR. In their work, CR and PRD were obtained of value 15.09 and 3.02, using both of these techniques and 7.31 and 2.8, using only HOSVD. A great improvement of their work was reflected in [19] by implementing multiscale HOSVD resulting in maximum CR of 45 and minimum PRD of 2.01. Though in this work, PRD hiked more than 25%, mainly in augmented limb leads. In [20], authors used MS-SVD on MECG data introducing new thresholding technique to select dominant singular values. The CR was achieved of 19.34 in their work along with PRD of 3.94. In [23], authors implemented 2D PCA upon beat matrix, to reduce interlead redundancy. To ensure quality controlled compression,

Table 2
Compression Result on PTBDB Records.

n-beat Tensor	Annotation type	No. of records	Lead wise PRD												Overall PRD	Overall PRDN	Overall CR
			I	II	III	aVR	aVL	aVF	V1	V2	V3	V4	V5	V6			
	BBB [a]	17	4.22	3.38	7.74	3.18	6.05	4.47	4.17	3.7	3.46	3.97	3.5	5.06	4.49	4.41	23.6
	Heart failure	18	5.29	4.08	8.03	4.37	7	5.52	4.96	3.94	3.83	3.45	3.32	4.86	5.2	4.89	23.4
	Dysrhythmia	16	6.2	5.99	6.82	6.38	6.43	5.98	4.9	4.95	5.28	4.09	4.06	4.36	5.45	5.46	22.9
	Healthy Control	72	3.8	2.62	4.59	2.66	4.77	3.21	3.12	2.78	2.9	2.77	3.11	3.53	3.37	3.32	23
$n = 5$	Hypertrophy	7	3.73	2.14	3.52	2.25	5.34	2.85	2.67	2.77	2.26	2.29	2.46	2.92	3.07	3.07	22.6
	MI [b]	377	3.74	2.85	3.78	2.95	4.01	3.31	3.11	2.92	3.01	3.3	3.85	4.25	3.47	3.47	21.7
	Myocarditis	4	2.11	0.59	1.22	0.89	3.55	0.75	2.32	1.64	1.81	2.39	3.04	2.64	1.91	1.91	23.5
	Miscellaneous	29	6.02	4.14	5.27	5.85	6.54	4.17	5.59	4.4	4.13	4.26	4.91	5.35	5.09	5.1	22.5
	VHD [c]	6	4.57	2.54	4.96	2.78	6.01	3.17	3.07	3.6	3.67	3.72	3.42	3.42	3.74	3.75	21.5
	BBB	17	5.52	4.66	9.23	4.49	7.37	5.75	5.73	4.98	4.41	5.2	4.66	6.41	5.81	5.81	44.5
	Heart failure	18	6.74	5.52	9.63	5.92	8.38	6.94	6.85	5.49	5.38	4.82	4.4	5.89	6.68	6.33	44.8
	Dysrhythmia	16	9.01	9.16	10.22	9.75	9.72	8.99	7.19	7.36	7.59	6.04	5.99	6.21	8.13	8.11	43.8
	Healthy Control	72	4.92	3.64	5.84	3.64	5.95	4.23	4.24	3.79	3.83	3.72	4.08	4.52	4.43	4.37	43.4
$n = 10$	Hypertrophy	7	4.85	2.88	4.47	2.99	6.7	3.76	3.15	3.45	2.88	2.88	3.08	3.61	3.88	3.88	42
	MI	377	5.22	4.09	5.19	4.2	5.49	4.65	4.38	4.07	4.15	4.52	5.21	5.62	4.79	4.79	40.7
	Myocarditis	4	2.68	0.81	1.5	1.18	4.53	0.97	3.04	2.2	2.47	3.14	3.94	3.26	2.48	2.48	45.3
	Miscellaneous	29	8.72	6.1	6.89	8.44	8.38	5.81	7.92	6.25	5.8	5.74	6.74	7.24	7	7.01	43.3
	VHD	6	5.86	3.36	6.37	3.6	7.75	4.11	4.03	4.71	4.78	4.73	4.66	4.13	4.84	4.85	40
	BBB	17	6.2	5.32	10.08	5.26	8.24	6.11	6.51	5.34	4.84	5.99	5.01	6.78	6.44	6.31	61.3
	Heart failure	18	7.62	6.51	11.07	6.88	9.27	8.06	7.59	6.56	6.28	5.69	4.97	6.39	7.6	7.25	62.6
	Dysrhythmia	16	9.99	10.72	12.08	10.97	11.09	10.82	8.24	8.22	8.56	6.74	6.68	7.04	9.3	9.27	63.7
	Healthy Control	72	5.42	4	6.52	3.97	6.61	4.74	4.76	4.33	4.31	4.13	4.51	4.94	4.93	4.86	57.9
$n = 15$	Hypertrophy	7	5.26	3.36	5.21	3.19	7.68	4.43	3.43	3.77	3.18	3.23	3.42	3.9	4.34	4.34	55.7
	MI	377	5.78	4.55	5.8	4.65	6.15	5.2	4.93	4.63	4.71	5.15	5.9	6.26	5.37	5.37	53.9
	Myocarditis	4	2.44	0.84	1.57	1.25	4.83	1	3.43	2.4	2.69	3.49	4.53	3.65	2.71	2.71	61
	Miscellaneous	29	9.65	6.47	6.99	8.84	8.37	6.05	8.59	7.17	6.57	6.24	7.45	7.76	7.51	7.52	58.6
	VHD	6	6.61	3.53	7.04	4.02	8.63	4.35	4.45	5.04	5.01	5.23	5.18	4.49	5.3	5.3	52

[a] BBB: bundle branch Block.
[b] MI: myocardial infarction.
[c] VHD: vulvar heart disease.

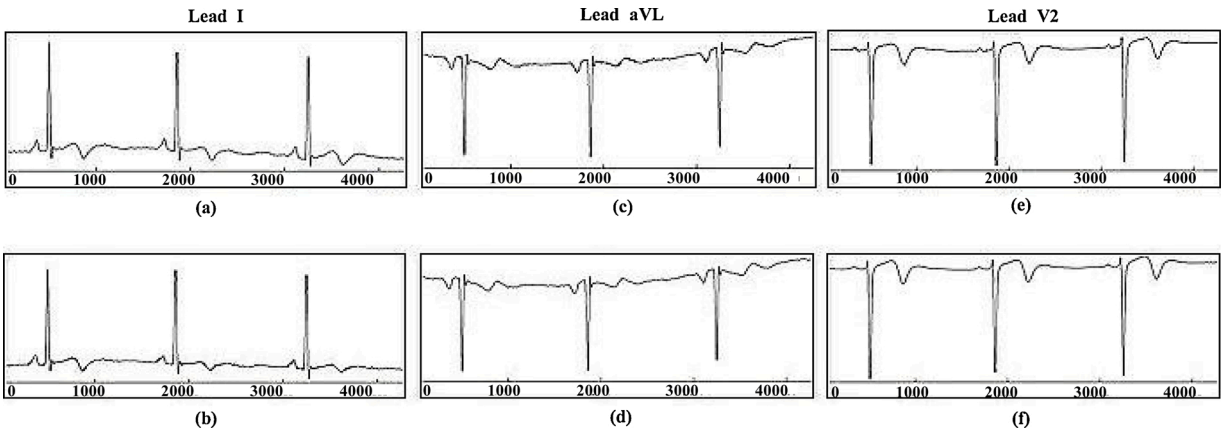

Fig. 5. Compression result on ptbdb data id 273s0511_re ('Myocardial Infarction') for 10 beat tensor decomposition with overall CR, PRD and PRDN of 53, 4.85 and 4.86, respectively; (a),(b) are the original and reconstructed signal of lead I respectively, with PRD of 5.21 ; (c),(d) are the original and reconstructed signal of lead aVL respectively, with PRD of 4; (e),(f) are the original and reconstructed signal of lead V2 respectively, with PRD of 3.91.

Table 3
Comparative Study with Recently Published Works.

Prior works	Quantization	Tool		CR	PRD	Description
A. E. Çetin et al., [11]	Fixed	DCT		6.17	6.19	Multi-channel ECG signal was first transformed to frequency domain coefficients using various linear transform techniques viz. DCT and KLT. Then, higher energy coefficients were compressed using subband coder and multirate transform coder was used to compress lower energy coefficients
		KLT		7.98		
A. G. Ramakrishnan et al., [12]	Fixed	DWT		18	11	After period and amplitude normalization, discrete wavelet transformed (DWT) was applied on ECG beats. Due to presence of high correlation between WT coefficients, the residue was stored with appropriate scaling factor, which was used for inverse WT during reconstruction.
J. Wei et al., [13]	Fixed	SVD		10	1.18	Authors applied singular value decomposition (SVD) on multi lead ECG to reduce redundancy. Higher energy singular vectors were preserved for reconstruction whereas, lower energy vectors were truncated to eliminate coherency at an aim of sufficient data compression
L. N. Sharma et al., [17]	Fixed	DWT and MSPCA		5.98	2.09	After selection of 8 independent leads, authors applied DWT on each of them. Then, upon all approximate and detailed coefficients, multi-scale PCA was implemented for dimension reduction. Then, Huffman coding was used to store the compressed data.
S. Padhy et al., [18]	Fixed	WT, HOSVD		15.09	3.02	After beat detection and period normalization, 3D beat tensor was formed. Authors achieved better compression result using higher order SVD (HOSVD) upon wavelet coefficients than using only HOSVD, on that 3 array data.
		HOSVD		7.31	2.8	
S. Padhy et al., [19]	Variable	WT and MS-HOSVD		>45 (max [a])	2.01 (min [b])	On MECG data, beta detection and period alignment was performed followed by tensor formation, using 10 successive beats. Then after WT, on each coefficient, multi-scale HOSVD (MS-HOSVD) was applied to compress the data. Though in this work, PRD hiked more than 25%, mainly in augmented limb leads.
S. Padhy et al., [20]	Fixed	MS-SVD		19.34	3.05	Authors applied multi-scale SVD on MECG data to reduce interlead and intrabeat redundancy. Then, a new approach of thresholding was proposed to select singular values. Finally after uniform quantization and Huffman coding, data was stored.
S. Banerjee et al., [23]	Optimal	PCA, PSO and MLP-NN		16.2	1.47	To reduce interlead redundancy, lead wise dimension reduction for each single beat, was proposed. Authors implemented PCA as data reduction tool. Finally PSO and multi-layer perceptron neural network (MLP-NN) based optimal quantization of each PC, was introduced to store compressed data.
S. Eftekharifar et al., [24]	Fixed	BSM and RCK		10	2.5-5.5	Authors introduced compressed sensing framework to reduce interlead redundancy. They implemented block space model (BSM), in collaboration with HiLasso reconstruction algorithm to compress the MECG data. They have also shown the better performance of raised cosine kernel (RCK), over Gaussian or WT, to generate the sparsifying basis matrices.
Proposed	**Optimal**	**TD, PCA, PSO, MASL**	**5-beat**	**22**	**3.62**	**At first Tucker Decomposition (TD) was applied on 3D beat tensor of '*n*' successive beats ('*n*' = 5, 10, 15). Then steganography was performed on PCs with least energy. A multi agent supervised learning (MASL) system was trained offline, using reference data which were previously optimized by a particle swarm optimization (PSO), to provide optimal quantization level to each PC to limit overall PRD within a specified value. Finally, after, delta and run length encoding, data was stored.**
			10-beat	**41.5**	**4.96**	
			15-beat	**55.4**	**5.59**	

[a] max: maximum.
[b] min: minimum.

MLP-NN based optimal quantization to each PC was proposed which resulted in CR and PRD of 16.2 and 1.47, respectively. In recent work, S. Eftekharifar et al. [24] proposed the block space model (BSM), in collaboration with HiLasso reconstruction algorithm to compress the MECG data. They obtained CR of 10 and variable PRD between 2.5 and 5.5.

As compared to previous works, in this proposed method, all the three types of redundancies were reduced using tensor decomposition

(Tucker decomposition) and lossless coding techniques. To encrypt patient's confidential information within the compressed ECG file, in this work first, steganography was proposed along with MECG data compression. To enhance the quality of compression, PSO and MASLS based optimal quantization, was also introduced. Finally, after implementing this algorithm upon MECG data, CR was of 22, 41.5, 55.4 and PRD of 3.62, 4.96, 5.59 were achieved using 5, 10, 15-beat tensor, respectively. In addition, due to implementation of optimal quantitation, the variation of PRD in each lead was almost similar (Table 2). The comparative study in Table 3 reveals that this algorithm provided better result as compared to other works.

This algorithm was also tested by formation of beat tensor using P and T-peak (i.e. in spite of creating a beat using corresponding R-peak, '*pseudo-beat*' was formed using P and T-peak) separately. For P-peak tensor, average CR, PRD and PRDN were achieved of value, 20.51, 4.12, 4.11 for 5 beat tensor, 42.6, 5.01, 5.12 for 10 beat tensor, and 56.1, 7.11, 7.34 for 15 beat tensor, respectively. Similarly, for T-peak tensor, mean CR, PRD and PRDN were computed as 22.2, 3.69, 4.02 for 5 beat tensor, 42, 4.98, 5.07 for 10 beat tensor, 54.2, 6.88, 7.01 for 15 beat tensor, respectively. But, while applying TD in beat tensor, the two end of each fiber, were more affected due to last sample padding and steganography, as compared to middle sections. Now, for P or T-peak tensor, the last two end contains fictitious domain of ECG like, P-wave, T-wave, QRS complex, hence effecting those features resulted in loss of clinical information. On the other hand, using R-peak tensor, the two end contains two successive TP-segments, which has very low clinical attributes. Thus it is always reliable to create the 3D tensor using each R-peak as reference point for quality improved performance.

5. Conclusion

The main objective of this proposed work, was to limit PRD within a specified value so that important characteristics of ECG would be almost unaffected after reconstruction ensuring enhanced quality compression process. Therefore, optimal quantization procedure was implemented, based on PSO and MASLS. The ANN was trained using features of 150 fibers or PCs, during testing period so that the PRD would be limited within 5%. Also to achieve high CR, 2D Tucker Decomposition was introduced using PCA, on 3D beat tensor which reduced the computation complexity. In order to maintain patient's privacy, data steganography was implemented along with the generation of 'secret key' to maintain authenticity. In 3-mode TD, though three redundancies would be reduced, but that was a time consuming procedure and needed much more buffer size. Therefore, only 2-mode PCA decomposition was performed to reduce the interbeat and interlead redundancies, whereas intrabeat redundancy was eliminated using double delta and run length encoding. This process also helped in steganography within core tensor by modifying the horizontal fibers with least energy. This algorithm was also tested on beat tensor created using P and T-peaks, separately ensuring this fact that this algorithm can be performed upon 3D tensor using any fixed reference point (i.e. either R, P or T-peaks). The compression result was also tested on 5, 10 and 15-beat tensor, so that it might be implemented on hardware devices (e.g. Raspberry Pi) depending upon system requirements, in order to work using real-time data. It was also observed that average time needed for compression for 5, 10, and 15 beat tensor were 32.01, 16.39 and 12.74 microsecond per sample computation, respectively. Reconstruction was performed by reverse algorithm of compression, and if decryption of patient's information was necessary, user must provide proper 'secret key'. In this algorithm, though CR improves, the computational complications also increases with the increment of number of beats used to form beat tensor. In addition, a proper R-peak detection is necessary for creation of beat tensor, so that minimum distortion occurs in the important features of ECG.

Formatting of funding sources

This research did not receive any specific grant from funding agencies in the public, commercial, or not-for-profit sectors.

CRediT authorship contribution statement

Soumyendu Banerjee: Writing - original draft, Data curation, Methodology, Software, Validation. **Girish Kumar Singh:** Conceptualization, Visualization, Investigation, Supervision, Writing - review & editing.

Declaration of Competing Interest

The authors reported no declarations of interest.

References

[1] R. Gupta, M. Mitra, J. Bera, ECG Acquisition and Automated Remote Processing, Springer India, New Delhi, 2014, https://doi.org/10.1007/978-81-322-1557-8.
[2] R. Gupta, J.N. Bera, M. Mitra, An intelligent telecardiology system for offline wireless transmission and remote analysis of ECG, J. Med. Eng. Technol 36 (7) (2012) 358–365, https://doi.org/10.3109/03091902.2012.712200.
[3] Z.A.A. Alyasseri, A.T. Khader, M.A. Al-Betar, A.K. Abasi, S.N. Makhadmeh, EEG signals denoising using optimal wavelet transform hybridized with efficient metaheuristic methods, IEEE Access 8 (2020) 10584–10605, https://doi.org/10.1109/access.2019.2962658.
[4] Z.A.A. Alyasseri, A.T. Khader, M.A. Al-Betar, L.M. Abualigah, ECG signal denoising using β-hill climbing algorithm and wavelet transform, Proc 2017 8th Intern. Conf. Inform. Tech. (ICIT) (2017) 96–101, https://doi.org/10.1109/ICITECH.2017.8079971.
[5] Z.A.A. Alyasseri, A.T. Khader, M.A. Al-Betar, M.A. Awadallah, Hybridizing β-hill climbing with wavelet transform for denoising ECG signals, Inform. Sci. 429 (2018) 229–246, https://doi.org/10.1016/j.ins.2017.11.026.
[6] S.M. Jalaleddine, C.G. Hutchens, R.D. Strattan, W. Coberly, ECG data compression techniques-a unified approach, IEEE Trans. Biomed. Eng 37 (4) (1990) 329–342, https://doi.org/10.1109/10.52340.
[7] T. Tekeste, H. Saleh, B. Mohammad, M. Ismail, Ultra-Low power QRS detection and ECG compression architecture for IoT healthcare devices, IEEE Trans. Cir. Syst. 66 (2) (2019) 669–679, https://doi.org/10.1109/TCSI.2018.2867746.
[8] P. Kovács, S. Fridli, F. Schipp, Generalized rational variable projection with application in ECG compression, IEEE Trans. Sig. Proc. 68 (2020) 478–492, https://doi.org/10.1109/TSP.2019.2961234.
[9] J. Pan, W.J. Tompkins, A Real-Time QRS detection algorithm, IEEE Trans. Biomed. Eng. BME-32 (3) (1985) 230–236, https://doi.org/10.1109/TBME.1985.325532.
[10] B.U. Kohler, C. Hennig, R. Orglmeister, The principles of software QRS detection, IEEE Eng. Med. Biol. 6 (1) (2002) 42–57, https://doi.org/10.1109/51.993193.
[11] A.E. Çetin, H. Köymen, M.C. Aydin, Multichannel ECG data compression by multirate signal processing and transform domain coding techniques, IEEE Trans. Biomed. Eng. 40 (5) (1993) 495–499, https://doi.org/10.1109/10.243411.
[12] A.G. Ramakrishnan, S. Saha, ECG coding by wavelet-based linear prediction, IEEE Trans. Biomed. Eng. 44 (12) (1997) 1253–1261, https://doi.org/10.1109/10.649997.
[13] J. Wei, C. Chang, N. Chou, G. Jan, ECG data compression using truncated singular value decomposition, IEEE Trans. Inform. Tech. Biomed. 5 (4) (2001) 290–299, https://doi.org/10.1109/4233.966104.
[14] Jian Yang, Two-Dimensional Pca: a new approach to appearance-based face representation and recognition, IEEE Trans. Pat. Anal. Mach. Intel 26 (1) (2004) 131–137, https://doi.org/10.1109/TPAMI.2004.1261097.
[15] P. Langley, E.J. Bowers, A. Murray, Principal component analysis as a tool for analyzing beat-to-beat changes in ECG features: application to ECG-derived respiration, IEEE Trans. Biomed. Eng. 57 (4) (2010) 821–829, https://doi.org/10.1109/TBME.2009.2018297.
[16] L.N. Sharma, S. Dandapat, A. Mahanta, Multiscale entropy based multiscale principal component analysis for multichannel ECG data reduction, Proc. of the tenth IEEE Intern. Conf. Inform. Tech. Appl. Biomed., Corfu (2010) 1–4, https://doi.org/10.1109/ITAB.2010.5687778.
[17] L.N. Sharma, S. Dandapat, A. Mahanta, Multichannel ECG data compression based on multiscale principal component analysis, IEEE Trans. Inform. Tech. Biomed. 16 (4) (2012) 730–736, https://doi.org/10.1109/TITB.2012.2195322.
[18] S. Padhy, S. Dandapat, A new multilead ECG data compression method using higher-order singular value decomposition, Proc. of Twentieth Nation. Conf. Commun., Kanpur, India (2014), https://doi.org/10.1109/NCC.2014.6811355.
[19] S. Padhy, S. Dandapat, Exploiting multi-lead electrocardiogram correlations using robust third-order tensor decomposition, Health. Tech. Lett. 2 (5) (2015) 112–117, https://doi.org/10.1049/htl.2015.0020.
[20] S. Padhy, L.N. Sharma, S. Dandapat, Multilead ECG data compression using SVD in multiresolution domain, Biomed. Sig. Proc. Cont. 23 (2016) 10–18, https://doi.org/10.1016/j.bspc.2015.06.012.

[21] C. Hernando-Ramiro, M. Blanco-Velasco, L. Lovisolo, F. Cruz- Roldán, Consistent quality control in ECG compression by means of direct metrics, Physiol. Meas. 36 (9) (2015) 1981–1994, https://doi.org/10.1088/0967-3334/36/9/1981.
[22] R. Gupta, Quality aware compression of electrocardiogram using principal component analysis, J. Med. Syst. 40 (5) (2016) 1–11, https://doi.org/10.1007/s10916-016-0468-7.
[23] S. Banerjee, R. Gupta, J. Saha, Compression of multilead electrocardiogram using principal component analysis and machine learning approach, Proc. of IEEE Appl. Sig. Proc. Conf. (ASPCON), Kolkata, India (2018) 24–28, https://doi.org/10.1109/ASPCON.2018.8748572.
[24] S. Eftekharifar, T.Y. Rezaii, S. Beheshti, S. Daneshvar, Block sparse multi-lead ECG compression exploiting between-lead collaboration, IET Sig. Proc. 13 (1) (2019) 46–55, https://doi.org/10.1049/iet-spr.2018.5076.
[25] J. Fridrich, Steganography in Digital Media: Principles, Algorithms, and Applications, Cambridge University Press, United Kingdom, 2009, https://doi.org/10.1017/CBO9781139192903.
[26] A. Ibaida, I. Khalil, Wavelet-based ECG steganography for protecting patient confidential information in point-of-care systems, IEEE Trans. Biomed. Eng. 60 (12) (2013) 3322–3330, https://doi.org/10.1109/TBME.2013.2264539.
[27] K. Tseng, X. He, W. Kung, S. Chen, M. Liao, H. Huang, Wavelet-based watermarking and compression for ECG signals with verification evaluation, Sensors 14 (2) (2014) 3721–3736, https://doi.org/10.3390/s140203721.
[28] M. Raeiatibanadkooki, S.R. Quchani, M. Khalilzade, K. Bahaadinbeigy, Compression and encryption of ECG signal using wavelet and chaotically huffman code in telemedicine application, J. Med. Syst. 40 (3) (2016), https://doi.org/10.1007/s10916-016-0433-5.
[29] Q. Li, C. Rajagopalan, G.D. Clifford, Ventricular fibrillation and tachycardia classification using a machine learning approach, IEEE Trans. Biomed. Eng. 61 (6) (2014) 1607–1613, https://doi.org/10.1109/TBME.2013.2275000.
[30] S.M. Abubakar, W. Saadeh, M.A.B. Altaf, A wearable long-term single-lead ECG processor for early detection of cardiac arrhythmia, Proc. of the Desi. Autom. Tes. Eur. Conf. Exh. (DATE), Dresden (2018) 961–966, https://doi.org/10.23919/DATE.2018.8342148.
[31] J. Malmivuo, R. Plonsey, Bioelectromagnetism - Principles and Applications of Bioelectric and Biomagnetic Fields, Oxford University Press, New York, 1995, https://doi.org/10.1093/acprof:oso/9780195058239.001.0001.
[32] S. Banerjee, A first derivative based r-peak detection and DWT based beat delineation approach of single lead electrocardiogram signal, Proc. of IEEE Reg 10 Symp (TENSYMP), Kolkata, India (2019) 565–570, https://doi.org/10.1109/TENSYMP46218.2019.8971094.
[33] P. Kroonenberg, J. Leeuw, Principal component analysis of three-mode data by means of alternating least squares algorithms, Psychometrika 45 (1) (1980) 69–97, https://doi.org/10.1007/BF02293599.
[34] T. Kolda, B. Bader, Tensor decompositions and applications, SIAM Rev. 51 (3) (2009) 455–500, https://doi.org/10.1137/07070111X.
[35] A. Cichocki, D. Mandic, A.-H. Phan, C. Caiafa, G. Zhou, Q. Zhao, L. Lathauwer, Tensor decompositions for signal processing applications: from two-way to multiway component analysis, IEEE Sig. Proc. Mag. 32 (2) (2015) 145–163, https://doi.org/10.1109/MSP.2013.2297439.
[36] H. Lu, K. Plataniotis, A. Venetsanopoulos, MPCA: multilinear principal component analysis of tensor objects, IEEE Trans. Neu. Net. 19 (1) (2008) 18–39, https://doi.org/10.1109/TNN.2007.901277.
[37] S. Padhy, S. Dandapat, Third-order tensor based analysis of multilead ecg for classification of myocardial infarction, Biomed. Sig. Proc. Cont. 31 (2017) 71–78, https://doi.org/10.1016/j.bspc.2016.07.007.
[38] Y. Taguchi, Tensor decomposition-based and principal-component-analysis-based unsupervised feature extraction applied to the gene expression and methylation profiles in the brains of social insects with multiple castes, BMC Bioinformatics 19 (S4) (2018), https://doi.org/10.1186/s12859-018-2068-7.
[39] C. Lu, J. Feng, Y. Chen, W. Liu, Z. Lin, S. Yan, Tensor robust principal component analysis with a new tensor nuclear norm, IEEE Trans. Pat. Anal. Mach. Intel. 42 (4) (2020) 925–938, https://doi.org/10.1109/TPAMI.2019.2891760.
[40] C. Li, S. Yang, T.T. Nguyen, A self-learning particle swarm optimizer for global optimization problems, IEEE Trans. Sys. Man Cyber. Part B (Cybernetics) 42 (3) (2012) 627–646, https://doi.org/10.1109/TSMCB.2011.2171946.
[41] Y. Zhang, S. Wang, G. Ji1, A comprehensive survey on particle swarm optimization algorithm and its applications, Artif. Intel. Appl. 2015 (2015) 1–38, https://doi.org/10.1155/2015/931256.
[42] S.N. Makhadmeh, A.T. Khader, M.A. Al-Betar, S. Naim, Z.A.A. Alyasseri, A. K. Abasi, Particle swarm optimization algorithm for power scheduling problem using smart battery, Proc. 2019 IEEE Jord. Intern. Joi. Conf. Elec. Eng. Inform. Tech. (JEEIT) (2019) 672–677, https://doi.org/10.1109/jeeit.2019.8717468. Amman, Jordan.
[43] M.A. Sohail, Z. Taufique, S.M. Abubakar, W. Saadeh, M.A. Bin Altaf, An ECG processor for the detection of eight cardiac arrhythmias with minimum false alarms, 2019 IEEE Biomedical Circuits and Systems Conference (BioCAS), Nara, Japan (2019) 1–4, https://doi.org/10.1109/BIOCAS.2019.8919053.
[44] Z. Ebrahimi, M. Loni, M. Daneshtalab, A. Gharehbaghi, A review on deep learning methods for ECG arrhythmia classification, Expert Systems with Applications: X 7 (2020), https://doi.org/10.1016/j.eswax.2020.100033.
[45] A. Dimeas, N. Hatziargyriou, Operation of a multiagent system for microgrid control, IEEE Trans. Pow. Syst. 20 (3) (2005) 1447–1455, https://doi.org/10.1109/TPWRS.2005.852060.
[46] S.J. Russell, Artificial Intelligence: A Modern Approach, Pearson, Harlow, 2016, https://doi.org/10.5555/1671238g.
[47] Panait, S. Luke, Cooperative multi-agent learning: the state of the art, Auton. Age. Multi-Age. Syst. 11 (3) (2005) 387–434, https://doi.org/10.1007/s10458-005-2631-2.
[48] T. Liu, K. Lin, H. Wu, ECG data encryption then compression using singular value decomposition, IEEE Journ. Biomed. Heal. Inform. 22 (3) (2018) 707–713, https://doi.org/10.1109/JBHI.2017.2698498.
[49] "Physionet.org." [Online]. Available: www.physionet.org//https://physionet.org/.
[50] M. Blanco-Velasco, F. Cruz-Roldán, J. Godino-Llorente, J. Blanco-Velasco, C. Armiens-Aparicio, F. López-Ferreras, On the use of PRD and CR parameters for ECG compression, Med. Eng. Phys. 27 (9) (2005) 798–802, https://doi.org/10.1016/j.medengphy.2005.02.007.